

## Surface-enhanced correlations between polarised photons in resonance fluorescence

Henk F Arnoldus and Thomas F George

Departments of Physics & Astronomy and Chemistry, 239 Fronczak Hall, State University of New York at Buffalo, Buffalo, NY 14260, USA

Received 13 April 1987, in final form 14 September 1987

**Abstract.** Correlations between photons emitted by an atom in a laser field and near a metal surface are studied. With polarisation-dependent detection it is feasible to select photons which are emitted in a specific transition between degenerate substates. Both the Einstein coefficient for spontaneous decay of a particular excited substate and its branching towards the various ground states depend on the distance between the atom and the surface. A combination of these notions to design a geometry for the correlated detection of polarised photons is employed, in order to predict a strong dependence of the correlation functions on the atom-surface distance. In general, an enhancement of the correlations between emitted photons due to the presence of the metal surface is found if the atom-surface distance is (roughly) less than 20% of the wavelength of the fluorescence radiation. In particular the correlations between circularly polarised photons with the same helicity are modified dramatically, and the correlation time tends to infinity if the atom approaches the surface. It is pointed out how the different photon correlations can be understood from a simple interpretation of transition diagrams.

### 1. Introduction

Atoms near a metal surface have different optical properties than in free space. When an excited atom decays spontaneously to a lower state, it emits a fluorescent photon, which travels away from the atom. In the presence of an optically active boundary the photon can be reflected and then return to the atom, which experiences it as an external field. Stimulated absorption of this photon then effectively enhances the lifetime of the excited state since the net result is no emission at all. From a slightly different point of view we can regard the combination of atom and surface (induced charges and currents) as the system which actually decays under emission of a photon. Inhibition of the emission of photons is then considered as a consequence of the fact that radiation energy is temporarily stored in between the atom and the surface (photons travelling back and forth). In a third perspective we can say that the vacuum field in the half space above the surface is different from a vacuum field in empty space. Since it is the coupling between the atomic dipole moment and the empty modes of the electromagnetic field which provides the mechanism for spontaneous decay, it is obvious that the presence of a metal surface affects the decay process. This variety of interpretations about the mechanism of alteration of lifetimes is reminiscent of the discussion about self-reaction versus vacuum fluctuations, concerning the spontaneous decay of an atom in free space (Milonni *et al* 1973, Dalibard *et al* 1982, 1984).

Experimental evidence for a molecule-surface distance dependence of a lifetime was first found by Drexhage (1974) for molecular dye layers on a dielectric. Then Kleppner (1981) proposed to consider transitions between atomic Rydberg states, where the atom is confined in a high- $Q$  cavity or waveguide. These experiments were carried out, and cavity-enhanced spontaneous emission was observed by Goy *et al* (1985), and Hulet *et al* (1985) reported inhibition of the decay. Very recently a suppressed spontaneous decay was observed for an optical transition in caesium (Jhe *et al* 1987). The change of lifetime was brought about by passing the atomic beam through a tunnel of parallel mirrors. Calculations of lifetimes are numerous. We mention the early work of Morawitz (1969) concerning the decay of a two-level atom near a mirror and the extensions by Milonni and Knight (1973) to an atom in between two mirrors. More general approaches were developed by Agarwal (1974, 1975), including arbitrarily shaped dielectric substrates. Critical comments about the two-level model were made by Barton (1974).

We consider an atom near a metal surface and impose the limit of infinite conductivity. This pertains to the situation in the quoted experiments, where a surface reflectivity of about 96% could be achieved. Rather than obtaining information about the atom-surface interaction through the observation of the decay of the excited state, it should also be feasible to probe the system by a laser. With a cw laser we can conceivably drive a specific atomic transition and study the resonance fluorescence. A first advantage is that this method is in principle stationary, which implies that we can improve the statistics of a measurement by increasing the observation time. Secondly, the procedure is more flexible, since a variety of properties of the fluorescence can be measured, which all carry specific information about the radiating system. Lin *et al* (1983), Huang *et al* (1984) and Huang and George (1984) calculated the spectral distribution of the radiation emitted by a two-state atom. We shall consider the temporal correlations between fluorescent photons, detected with a well defined polarisation and emitted by a degenerate two-level atom. In a previous paper (Arnoldus and George 1987) we studied the case where the atom effectively behaves as a two-state system, which can be managed by choosing a specific atomic transition and laser polarisation. We now extend our calculations to the situation where the atom is essentially a multilevel atom, which opens a variety of new possibilities. After the general theory in §§ 2-4, we shall elaborate on the case  $j_e = j_g = \frac{1}{2}$ , which generalises the results for atoms in free space (Cohen-Tannoudji and Reynaud 1979).

## 2. Spontaneous decay

An atom is positioned at a distance  $h$  above a perfect conductor. Two degenerate levels, which are in close resonance with the incident laser field will be denoted by  $|j_e m_e\rangle$  (excited) and  $|j_g m_g\rangle$  (ground), and they have energies  $\hbar\omega_e$  and  $\hbar\omega_g$ , respectively, with  $\omega_0 = \omega_e - \omega_g > 0$ . The significance of the magnetic quantum numbers  $m_e$  and  $m_g$  is fixed as soon as an atomic quantisation axis is prescribed. A convenient choice is the direction perpendicular to the surface, indicated by the  $z$  axis, and the solid will be assumed to occupy the half space  $z < 0$ . Then the Einstein coefficient for spontaneous decay (inverse lifetime) of the substate  $|j_e m_e\rangle$  is given by (Arnoldus and George 1987)

$$A_{m_e} = A_f \sum_{\tau} b_{\tau}(\omega_0 h/c) \sum_{m_g} (j_g m_g 1 \tau | j_e m_e)^2 \quad (2.1)$$

where  $\tau$  takes on the values  $-1, 0, 1$ . The functions  $b_{\tau}$ , which embody the distance

dependence of the lifetimes, are explicitly

$$b_0(x) = 1 - 3 \left( \frac{\cos(2x)}{(2x)^2} - \frac{\sin(2x)}{(2x)^3} \right) \quad (2.2)$$

$$b_{\pm 1}(x) = 1 - \frac{3}{2} \left( \frac{\sin(2x)}{2x} + \frac{\cos(2x)}{(2x)^2} - \frac{\sin(2x)}{(2x)^3} \right) \quad (2.3)$$

and they approach unity for  $x = \omega_0 h/c \rightarrow \infty$ . In that situation we find from the orthogonality relations for Clebsch-Gordan coefficients that  $A_{m_e} = A_f$ . Hence every substate decays with the same rate constant

$$A_f = \frac{\omega_0^3}{3\pi\epsilon_0 \hbar c^3} \frac{|\langle j_e \parallel \mu \parallel j_g \rangle|^2}{2j_e + 1} \quad (2.4)$$

expressing the isotropy of fluorescent emission by free atoms. Near a surface the substates have different Einstein coefficients, and from  $b_{+1} = b_{-1}$  we find the relation

$$A_{m_e} = A_{-m_e} \quad (2.5)$$

as a result of the remaining cylindrical symmetry around the  $z$  axis. Non-vanishing Clebsch-Gordan coefficients in equation (2.1) obey the relation  $m_g + \tau = m_e$ . Therefore, an  $|m_e - m_g| = 1$  transition has an atom-surface-dependent Einstein coefficient, which is governed by  $b_{\pm 1}(\omega_0 h/c)$ , whereas an  $|m_e - m_g| = 0$  transition constant is proportional to  $b_0(\omega_0 h/c)$ . Contributions to  $A_{m_e}$  with  $\tau = \pm 1$  originate from the parallel components, with respect to the surface, of the atomic dipole operator  $\mu$ , whereas the  $\tau = 0$  term comes from the perpendicular component. For this reason we distinguish between two fundamental Einstein coefficients in the vicinity of a perfect conductor:

$$A_{\perp} = A_f b_0(\omega_0 h/c) \quad A_{\parallel} = A_f b_{\pm 1}(\omega_0 h/c) \quad (2.6)$$

which both tend to  $A_f$  for  $h \rightarrow \infty$ . From (2.1) we then find the sum rule

$$(2j_e + 1)^{-1} \sum_{m_e} A_{m_e} = \frac{1}{3} A_{\perp} + \frac{2}{3} A_{\parallel} \quad (2.7)$$

for the average decay constant.

Spontaneous decay of the atom gives rise to a damping of its density operator  $\sigma(t)$  in a time evolution. This relaxation is most conveniently accounted for by a Liouville operator  $\Gamma$ , which acts on  $\sigma$  according to (Arnoldus and George 1987)

$$\begin{aligned} \Gamma \sigma = & \frac{1}{2} \sum_{m_e} A_{m_e} (|j_e m_e\rangle \langle j_e m_e| \sigma + \sigma |j_e m_e\rangle \langle j_e m_e|) \\ & - A_f \sum_{\tau} b_{\tau}(\omega_0 h/c) \sum_{\substack{m_e m_g \\ m'_e m'_g}} \langle j_e m_e | \sigma | j_e m'_e \rangle \langle j_g m_g 1 \tau | j_e m_e \rangle \\ & \times \langle j_g m'_g 1 \tau | j_e m'_e \rangle | j_g m_g \rangle \langle j_g m'_g |. \end{aligned} \quad (2.8)$$

### 3. Laser-driven system

A laser field with central frequency  $\omega_L$ , polarisation  $\epsilon$ , wavevector  $\mathbf{k}$  (with  $\mathbf{k} \cdot \epsilon = 0$ ), amplitude  $E_0$  and linewidth  $\lambda$  is incident upon the surface. This radiation reflects on the surface, and the sum of incident and reflected fields evaluated at  $h\mathbf{e}_z$  equals the

external field, which is experienced by the atom. In terms of the projectors onto the excited state and ground state

$$P_i = \sum_{m_i} |j_i m_i\rangle \langle j_i m_i| \quad i = e, g \quad (3.1)$$

the dipole coupling can be expressed in terms of a 'Rabi operator'

$$\Omega(h) = \hbar^{-1} E_0 P_e (\boldsymbol{\mu}_s (h\mathbf{k} \cdot \mathbf{e}_z) \cdot \boldsymbol{\varepsilon}) P_g \quad (3.2)$$

which involves an effective (non-Hermitian) dipole moment

$$\boldsymbol{\mu}_s(x) = 2 \cos(x) \boldsymbol{\mu}_\perp + 2i \sin(x) \boldsymbol{\mu}_\parallel. \quad (3.3)$$

Here, the atomic dipole moment  $\boldsymbol{\mu}$  is divided into a perpendicular and parallel part with respect to the surface. This laser-atom interaction introduces the second atom-surface distance dependence in the problem, although in a rather trivial way. The Hamiltonian which governs the behaviour of the atom in the external field can now be written as

$$H_d = \hbar\omega_e P_e + \hbar(\omega_g + \omega_L) P_g - \frac{1}{2} \hbar (\Omega(h) + \Omega(h)^\dagger) \quad (3.4)$$

where this  $H_d$  is usually referred to as the dressed-atom Hamiltonian (Cohen-Tannoudji 1977).

In the compact Liouville formalism the equation of motion reads

$$i \frac{d\sigma}{dt} = (L_d - iW - i\Gamma)\sigma \quad (3.5)$$

for the atomic density operator in the rotating frame (Allen and Eberly 1975). Spontaneous decay is incorporated in  $\Gamma$  (equation (2.8)), the free evolution of the dressed atom is represented by

$$L_d \sigma = \hbar^{-1} [H_d, \sigma] \quad (3.6)$$

and the relaxation operator  $W$ , which accounts for the laser linewidth, is given by (Agarwal 1978)

$$W\sigma = \lambda (P_g \sigma + \sigma P_g - 2P_g \sigma P_g) \quad (3.7)$$

where  $\lambda$  is the halfwidth at half maximum of the Lorentzian laser profile.

Of particular importance is the long-time solution, or steady state, which obeys

$$(L_d - iW - i\Gamma)\bar{\sigma} = 0 \quad \bar{\sigma}^\dagger = \bar{\sigma} \quad \text{Tr } \bar{\sigma} = 1 \quad (3.8)$$

where we have indicated  $\sigma(t = \infty)$  by  $\bar{\sigma}$ .

For later purposes we write down the matrix elements of the Rabi operator  $\Omega(h)$ . Due to the appearance of the projectors in equation (3.2), the only possibly non-vanishing matrix elements are

$$\begin{aligned} \langle j_e m_e | \Omega(h) | j_g m_g \rangle = & \hbar^{-1} E_0 (2j_e + 1)^{-1/2} \langle j_e \| \boldsymbol{\mu} \| j_g \rangle \left( 2 \cos(hk_z) (\mathbf{e}_z \cdot \boldsymbol{\varepsilon}) \langle j_g m_g 1 0 | j_e m_e \rangle \right. \\ & \left. + 2i \sin(hk_z) \sum_{\tau=\pm 1} (\mathbf{e}_\tau^* \cdot \boldsymbol{\varepsilon}) \langle j_g m_g 1 \tau | j_e m_e \rangle \right) \end{aligned} \quad (3.9)$$

with  $k_z = \mathbf{k} \cdot \mathbf{e}_z$ , and in terms of the spherical unit vectors with respect to the  $z$  axis

$$\mathbf{e}_{\pm 1} = \mp (\mathbf{e}_x \pm i\mathbf{e}_y) / \sqrt{2}. \quad (3.10)$$

Then zero Clebsch-Gordan coefficients for particular values of  $j_e$ ,  $m_e$ ,  $j_g$ ,  $m_g$  express the dipole selection rules.

#### 4. Photon detection

Temporal correlations between photons in an electromagnetic field can be understood most easily from the theory of photon detection by a photomultiplier tube (PM), as developed by Glauber (1965) and Kelley and Kleiner (1964). Polarisation-dependent measurements can be performed by putting a polariser in front of the PM, which only transmits the  $e_\alpha$  component of the incident radiation. In the case under consideration, we position a PM with polariser  $e_\alpha$  in the region  $z > 0$  in such a way that the propagation direction  $\hat{r}$  of the fluorescence which ends up in the detector is perpendicular to  $e_\alpha$ . Then there is a simple relationship between the detection of a photon with polarisation  $e_\alpha$  and its emission in the direction  $\hat{r}$ . For an atom near a perfect conductor we find, with a slight generalisation of Arnoldus and Nienhuis (1983), that the photon-emission operator  $R_\alpha$  equals

$$R_\alpha \sigma = \sum_{\substack{m_e m_g \\ m'_e m'_g}} |j_g m_g\rangle \langle j_g m'_g| \langle j_e m_e | \sigma | j_e m'_e \rangle \\ \times \langle j_e m_e | \mu_s(\omega_0 \tau_d) \cdot e_\alpha | j_g m_g \rangle^* \langle j_e m'_e | \mu_s(\omega_0 \tau_d) \cdot e_\alpha | j_g m'_g \rangle \quad (4.1)$$

which defines its action on an arbitrary atomic density operator  $\sigma$ . The appearance of  $\mu_s(\omega_0 \tau_d)$ , rather than the dipole operator  $\mu$  itself (as for a free atom), represents the interference between photons which travel directly from the atom to the detector and photons which are first reflected by the surface. Here,  $\tau_d = c^{-1} \hat{r} \cdot h e_z$  equals half the delay time of a reflected photon.

We shall always assume that the atom has been in the laser field for a sufficiently long time, so that  $\sigma(t)$  has reached its steady state  $\bar{\sigma}$ . Then the number of detected photons per unit of time with polarisation  $e_\alpha$  is proportional to the expectation value of  $R_\alpha$ . We write for this counting rate or intensity

$$I_\alpha = \zeta_\alpha \text{Tr } R_\alpha \bar{\sigma} \quad (4.2)$$

where  $\zeta_\alpha$  is a detector parameter, depending on the efficiency, transmission factor of the polariser, aperture, etc. We can evaluate  $I_\alpha$  immediately for any configuration as soon as we have solved equation (3.8) for  $\bar{\sigma}$ .

More interesting are the two-photon correlations. Suppose we have two detectors with polarisers  $e_\alpha$  and  $e_\beta$ . Then we can define the intensity correlation for the detection of two polarised photons as  $I_{\alpha\beta}(t_1, t_2) dt_1 dt_2$ , which is the probability for the detection of a photon with polarisation  $e_\alpha$  in  $[t_1, t_1 + dt_1]$  and the detection of a photon with polarisation  $e_\beta$  in  $[t_2, t_2 + dt_2]$ , irrespective of detections at other times. From the quoted detector theory it then follows that  $I_{\alpha\beta}$  equals

$$I_{\alpha\beta}(t_1, t_2) = \zeta_\beta \zeta_\alpha \text{Tr } R_\beta U(t_2 - t_1) R_\alpha \bar{\sigma} \quad t_2 \geq t_1 \quad (4.3)$$

in terms of the time-regression operator  $U(t)$  for the atomic-density operator. From equation (3.5) we find explicitly

$$U(t) = \exp[-i(L_d - iW - i\Gamma)t]. \quad (4.4)$$

The importance of the study of photon correlations is most obvious from expression (4.3). It is the time-evolution operator  $U(t)$  for the atom, including its interactions with the environment, which determines the time delay  $t_2 - t_1$  between two emissions. Therefore, dynamical properties of the radiating system will be reflected in the details of  $I_{\alpha\beta}(t_1, t_2)$ . The two-photon correlation functions have been measured for free sodium

atoms in a laser beam (Kimble *et al* 1977, 1978, Dagenais and Mandel 1978), and excellent agreement with theoretical predictions was found.

From definition (4.1) we readily find

$$R_\beta R_\alpha = 0 \quad \text{and} \quad I_{\alpha\beta}(t_1, t_1) = 0 \quad (4.5)$$

which displays the fact that emission of two photons with a zero time delay cannot occur in two-level atom resonance fluorescence. This phenomenon is termed antibunching of photons (Paul 1982). On the other hand, we find from the conservation of trace in a time evolution with  $U(t)$  the identity

$$\lim_{t \rightarrow \infty} U(t) R_\alpha \bar{\sigma} = \bar{\sigma} \text{Tr} R_\alpha \bar{\sigma} \quad (4.6)$$

which implies for the detection of two photons with a long time delay

$$I_{\alpha\beta}(t_1, t_1 + \infty) = I_\alpha I_\beta \quad (4.7)$$

i.e. the detections are uncorrelated. It is convention (Lenstra 1982) to introduce the normalised quantity

$$f_{\beta\alpha}(t) = I_{\alpha\beta}(t_1, t_1 + t) / I_\alpha \quad (4.8)$$

which has the significance of the probability for the detection of a photon with polarisation  $e_\beta$  at time  $t$ , after the detection of a photon with polarisation  $e_\alpha$  at time zero. Its short- and long-time values are

$$f_{\beta\alpha}(0) = 0 \quad f_{\beta\alpha}(\infty) = I_\beta \quad (4.9)$$

where the last equality states that for large  $t$  the memory of the emission of the  $e_\alpha$  photon at time zero is erased.

## 5. Geometry

It is the purpose of this paper to take advantage of the degeneracies of the atomic levels in combination with the option of detecting photons with a polarisation resolution, in order to obtain maximum information about atomic lifetimes near a metal surface through the process of photon counting (intensity and correlation). From (3.9) it follows that the simplest non-trivial (not effectively a two-level atom) coupling scheme arises for  $j_e = j_g = \frac{1}{2}$ . Then both atomic levels are twofold degenerate, and they will be abbreviated as  $|e\pm\rangle$  and  $|g\pm\rangle$  in a self-explanatory notation. We take  $\mathbf{k}$  in the  $xy$  plane (propagation along the surface), and a linear laser polarisation  $\boldsymbol{\varepsilon} = \mathbf{e}_z$ . For this configuration the  $\hbar$  dependence of  $\Omega(\hbar)$  disappears.

The polarisation dependence of photon detection is determined by matrix elements of

$$\boldsymbol{\mu}_s(\omega_0\tau_d) \cdot \mathbf{e}_\alpha = 2 \cos(\omega_0\tau_d) \boldsymbol{\mu}_\perp \cdot \mathbf{e}_\alpha + 2i \sin(\omega_0\tau_d) \boldsymbol{\mu}_\parallel \cdot \mathbf{e}_\alpha \quad (5.1)$$

with  $\tau_d = \hat{\mathbf{r}} \cdot \mathbf{e}_z \hbar / c$ , according to equation (4.1). For a PM in the  $xy$  plane we have  $\tau_d = 0$ , and (5.1) reduces to  $2\boldsymbol{\mu}_\perp \cdot \mathbf{e}_\alpha$ . Obviously, the disappearance of the contribution from  $\boldsymbol{\mu}_\parallel$  is a result of interference between directly emitted and reflected photons. With  $\boldsymbol{\mu}_\perp \cdot \mathbf{e}_\alpha = (\boldsymbol{\mu}_\perp \cdot \mathbf{e}_z)(\mathbf{e}_\alpha \cdot \mathbf{e}_z)$  we find that the only effect of the polariser is a contribution of a factor  $|\mathbf{e}_\alpha \cdot \mathbf{e}_z|^2$  in  $R_\alpha$ , and from that we conclude that the radiation is linearly polarised in the  $z$  direction. Therefore, we can choose  $\mathbf{e}_\alpha = \mathbf{e}_z$  without loss of generality.

Of course, the fact that the radiation is linearly polarised in the  $xy$  plane follows immediately from the boundary conditions near a perfect conductor. Subsequently we consider a PM on the  $z$  axis, for which expression (5.1) reduces to  $2i \sin(\omega_0 h/c) \mu_{\parallel} \cdot e_{\alpha}$ . Here we have to choose two independent polarisation directions  $e_{\alpha}$ , perpendicular to the  $z$  axis, which will be taken as the spherical unit vectors  $e_{\pm 1}$ . Photon-emission operators will be denoted by  $R_0$  (detection in the  $xy$  plane) and  $R_{\pm}$  (propagation direction of fluorescence perpendicular to the surface). Figure 1 illustrates and summarises the geometry and polarisations.

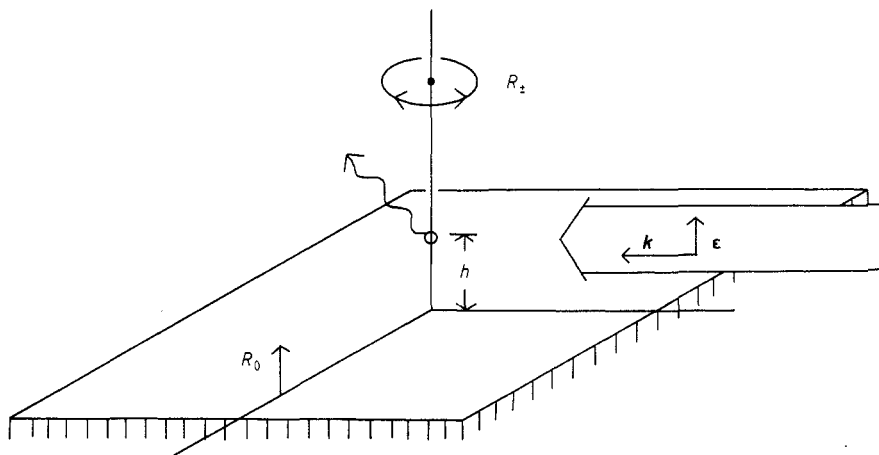


**Figure 1.** Schematic representation of the spatial configuration for the correlation measurement of polarised photons, which are emitted by an atom at a distance  $h$  above a perfectly conducting metal. A laser beam with wavevector  $k$  and polarisation  $\epsilon$  irradiates the atom, and the emitted fluorescence (wiggly arrow) is detected by a combination of photomultipliers and polarisers. The detector  $R_0$  in the  $xy$  plane has a linear polarisation filter, and the detectors  $R_{\pm}$  above the surface count circularly polarised photons.

The coupling strength with the laser field will be expressed in the Rabi frequency (complex number)

$$\Omega_0 = \hbar^{-1} E_0 \left(\frac{2}{3}\right)^{1/2} \langle e_{\parallel} | \mu | g \rangle. \quad (5.2)$$

Then the equation of motion (3.5) can easily be expanded in matrix elements to yield a set of 16 coupled linear first-order differential equations. Two of them read

$$\begin{aligned} \frac{d}{dt} \langle g_{\pm} | \sigma | g_{\pm} \rangle &= \frac{1}{3} A_{\perp} \langle e_{\pm} | \sigma | e_{\pm} \rangle \\ &+ \frac{2}{3} A_{\parallel} \langle e_{\mp} | \sigma | e_{\mp} \rangle \mp \frac{1}{2} i \Omega_0 \langle g_{\pm} | \sigma | e_{\pm} \rangle \pm \frac{1}{2} i \Omega_0^* \langle e_{\pm} | \sigma | g_{\pm} \rangle \end{aligned} \quad (5.3)$$

from which we deduce that the upper states  $|e_{\pm}\rangle$  decay to  $|g_{\pm}\rangle$  with Einstein coefficient  $A_{\perp}/3$ , and to  $|g_{\mp}\rangle$  with  $2A_{\parallel}/3$ . The total decay constants  $A_{\pm 1/2}$  for the upper states will be denoted by

$$A = \frac{1}{3} A_{\perp} + \frac{2}{3} A_{\parallel}. \quad (5.4)$$

Figure 2 illustrates the level configuration and the various couplings.

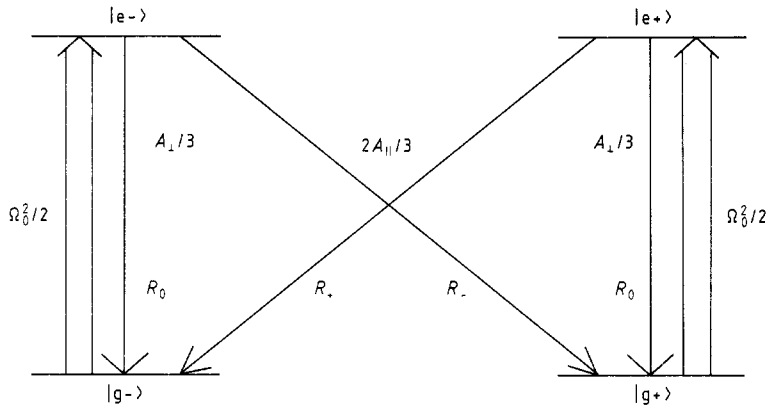


**Figure 2.** Level configuration for  $j_e = j_g = \frac{1}{2}$  and radiative transitions. Two double arrows indicate stimulated excitation by the laser, and the four single arrows represent spontaneous decay and photon emission. The geometry of figure 1 is designed in such a way that photons which are emitted in a transition denoted by  $R_+$ ,  $R_-$  or  $R_0$  are detected by the corresponding devices of figure 1.

Of relevance to the photon-detection probabilities are the populations of the excited states  $|e\pm\rangle$ , in the steady state. Solving equation (3.8) gives immediately

$$n_e = \langle e\pm | \bar{\sigma} | e\pm \rangle = \frac{\frac{1}{4} |\Omega_0|^2 (\frac{1}{2} A + \lambda)}{|\Omega_0|^2 (\frac{1}{2} A + \lambda) + A [(\frac{1}{2} A + \lambda)^2 + \Delta^2]} \tag{5.5}$$

and furthermore the population  $\langle g\pm | \bar{\sigma} | g\pm \rangle$ , and the coherences  $\langle e\pm | \bar{\sigma} | g\pm \rangle$  and  $\langle g\pm | \bar{\sigma} | e\pm \rangle$  acquire a finite value. The other eight matrix elements of  $\bar{\sigma}$  vanish identically. Here,  $\Delta = \omega_L - \omega_0$  is the detuning of the laser from resonance. Notice that the populations of the excited states depend only on the total Einstein coefficient  $A$ , rather than on  $A_\perp$  and  $A_\parallel$  separately. This can be understood from the fact that it does not matter for the populations of  $|e\pm\rangle$  to which ground state they decay.

From (4.1) we find the photon-emission operators for the three polarisation directions

$$R_\pm \sigma = 2 \sin^2(\omega_0 h/c) \langle e\pm | \sigma | e\pm \rangle |g\mp\rangle \langle g\mp| \tag{5.6}$$

$$R_0 \sigma = \sum_{m,m'=\pm} mm' \langle em | \sigma | em' \rangle |gm\rangle \langle gm'| \tag{5.7}$$

where a factor  $(\frac{2}{3}) |\langle e || \mu || g \rangle|^2$  is suppressed (can always be absorbed in  $\zeta_\alpha$ ). In equation (5.7) the coherences  $\langle e\pm | \sigma | e\mp \rangle$  appear. We already found that in the steady state  $\bar{\sigma}$  the coherences between two excited states vanish. As seen from equation (4.3), the emission operator  $R_\alpha$  always acts on  $\bar{\sigma}$ , which gives in the three cases

$$R_\pm \bar{\sigma} = 2 \sin^2(\omega_0 h/c) n_e |g\mp\rangle \langle g\mp| \tag{5.8}$$

$$R_0 \bar{\sigma} = n_e (|g+\rangle \langle g+| + |g-\rangle \langle g-|). \tag{5.9}$$

Then the time-evolution operator  $U(t)$  acts on these expressions, which effectively gives combinations of  $U(t) |g\pm\rangle \langle g\pm|$ . It is straightforward to show from the equation of motion in matrix form that the coherences between the excited states of  $\sigma(t) = U(t) |g\pm\rangle \langle g\pm|$  are zero for all  $t$ . A subsequent action of  $R_0$  then only involves the terms with  $m = m'$  in equation (5.7), so for every occurring  $R_0$  we can effectively take

$$R_0 \sigma = \sum_{m=\pm} \langle em | \sigma | em \rangle |gm\rangle \langle gm|. \tag{5.10}$$

Inspection of equation (5.6) reveals that the probability for the emission of a  $\pm$  photon is proportional to the population of the excited state  $|e\pm\rangle$ , and that after the emission the atom is left in the ground state  $|g\mp\rangle$ . Therefore, an emission of a  $\pm$  photon is accompanied by a transition  $|e\pm\rangle \rightarrow |g\mp\rangle$  by the atom. Similarly, we see from equation (5.10) that emissions of linearly polarised photons gain contributions from the two processes  $|e+\rangle \rightarrow |g+\rangle$  and  $|e-\rangle \rightarrow |g-\rangle$ . This interpretation is illustrated in figure 2. On the other hand, we know from the equation of motion (for instance (5.3)) that transitions  $|e\pm\rangle \rightarrow |g\mp\rangle$  occur at a rate  $n_e 2A_{\parallel}/3$ , whereas  $|e\pm\rangle \rightarrow |g\pm\rangle$  transitions happen  $n_e A_{\perp}/3$  times per unit of time. Every transition corresponds to the emission of a photon with a particular polarisation, and the corresponding counting rate  $I_{\alpha} = \zeta_{\alpha} \text{Tr } R_{\alpha} \bar{\sigma}$  must therefore be proportional to the emission rate. Comparison with expressions (5.8) and (5.9) then shows that we can write the detector parameters  $\zeta_{\alpha}$  as

$$\zeta_{\pm} 2 \sin^2(\omega_0 h/c) = \eta_{\pm} \frac{2}{3} A_{\parallel} \tag{5.11}$$

$$\zeta_0 = \eta_0 \frac{1}{3} A_{\perp} \tag{5.12}$$

where the dimensionless parameters  $\eta_{\alpha}$  have the significance of the probability that an emitted photon is detected.

Finally we obtain for the intensities

$$I_{\pm} = \eta_{\pm} \frac{2}{3} A_{\parallel} n_e \tag{5.13}$$

$$I_0 = 2\eta_0 \frac{1}{3} A_{\perp} n_e \tag{5.14}$$

in terms of  $n_e$  from equation (5.5). With (2.6) we then find

$$\frac{I_{\pm}}{I_0} = \frac{\eta_{\pm}}{\eta_0} \frac{A_{\parallel}}{A_{\perp}} = \frac{\eta_{\pm}}{\eta_0} \frac{b_{\pm}(\omega_0 h/c)}{b_0(\omega_0 h/c)} \tag{5.15}$$

which shows that the ratio of detected circularly polarised and linearly polarised photons depends only on the atom-surface distance  $h$  as  $b_{\pm}/b_0$ , independent of any other parameter (laser power, linewidth, dipole moment, etc), provided every emitted photon is detected. This universal curve is plotted in figure 3.

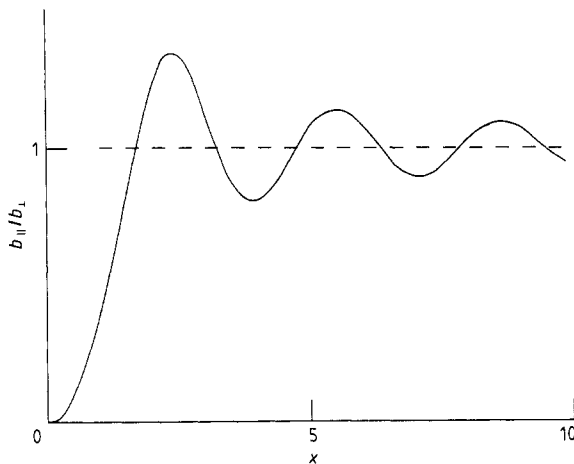


**Figure 3.** Ratio  $A_{\parallel}/A_{\perp}$  as a function of  $x = \omega_0 h/c$ , which equals the ratio of the number of emitted circularly polarised photons and linearly polarised photons. For  $h \rightarrow \infty$  this ratio approaches unity.

## 6. Photon correlations

In this section we evaluate the two-photon correlation functions  $f_{\beta\alpha}(t)$  from equation (5.9) for all possible combinations of  $\alpha = -1, 0, 1$  with  $\beta = -1, 0, 1$ . From (5.8) and (5.9) we observe that  $R_\alpha \bar{\sigma}$  is a combination of projectors  $|g_\pm\rangle\langle g_\pm|$ . These states evolve in time as  $U(t)|g_\pm\rangle\langle g_\pm|$ , and the subsequent action of  $R_\beta$  takes the excited-state populations of the result. Hence every  $f_{\beta\alpha}(t)$  can be expressed in the four functions

$$g_{mn}(t) = \langle en | (U(t) |gm\rangle\langle gm|) |en\rangle \quad (6.1)$$

with  $m = \pm$  and  $n = \pm$ . This  $g_{mn}(t)$  is simply the population of  $|en\rangle$  at time  $t$  if the atom is in the ground state  $|gm\rangle$  at time zero. In terms of the  $g_{mn}$ , the nine two-photon correlation functions become

$$f_{\pm\pm}(t) = \eta_{\pm} \frac{2}{3} A_{\parallel} g_{\pm\pm}(t) \quad (6.2)$$

$$f_{\mp\pm}(t) = \eta_{\mp} \frac{2}{3} A_{\parallel} g_{\mp\pm}(t) \quad (6.3)$$

$$f_{0\pm}(t) = \eta_0 \frac{1}{3} A_{\perp} (g_{\mp+}(t) + g_{\mp-}(t)) \quad (6.4)$$

$$f_{\pm 0}(t) = \eta_{\pm} \frac{2}{3} A_{\parallel} \frac{1}{2} (g_{-\pm}(t) + g_{+\pm}(t)) \quad (6.5)$$

$$f_{00}(t) = \eta_0 \frac{1}{3} A_{\perp} \frac{1}{2} (g_{++}(t) + g_{--}(t) + g_{+-}(t) + g_{-+}(t)). \quad (6.6)$$

Explicit evaluation of  $g_{mn}(t)$  is most conveniently done in the Laplace domain. We write

$$\tilde{g}_{mn}(s) = \int_0^{\infty} dt \exp(-st) g_{mn}(t) \quad (6.7)$$

and from a combination of (4.4) and (6.1) we obtain the formal result

$$\tilde{g}_{mn}(s) = \langle en | \left( \frac{1}{s + iL_d + W + \Gamma} |gm\rangle\langle gm| \right) |en\rangle \quad (6.8)$$

in terms of an operator inversion. In a matrix representation the operator  $s + iL_d + W + \Gamma$  is a  $16 \times 16$  matrix which has to be inverted. With some algebra we find

$$\tilde{g}_{mn}(s) = \frac{1}{4} |\Omega_0|^2 \left( \frac{1}{sD(s)} + \frac{mn}{sD(s) + |\Omega_0|^2 (\frac{1}{2}A + \lambda + s) 2A_{\parallel}/3} \right) \quad (6.9)$$

with

$$D(s) = |\Omega_0|^2 (\frac{1}{2}A + \lambda + s) + (A + s) [(\frac{1}{2}A + \lambda + s)^2 + \Delta^2]. \quad (6.10)$$

We notice that  $\tilde{g}_{mn}(s)$  depends only on  $m$  and  $n$  through the product  $mn$ , so we can express the four functions  $g_{mn}(t)$  in terms of the two functions

$$g_+(t) = g_{\pm\pm}(t) \quad (6.11)$$

$$g_-(t) = g_{\mp\mp}(t). \quad (6.12)$$

Their explicit form (in the Laplace domain) follows from equation (6.9) by setting  $mn = 1$  and  $mn = -1$ , respectively. Transformation of  $\tilde{g}_{\pm}(s)$  to the time domain is (numerically) trivial.

The functions  $f_{\beta\alpha}(t)$  (equations (6.2)–(6.6)) are proportional to an efficiency parameter  $\eta_\beta$  and an Einstein coefficient, which do not represent any dynamical properties of the system. They merely fix the long-time behaviour  $f_{\beta\alpha}(t) \rightarrow I_\beta$  for  $t \rightarrow \infty$ , so an appropriate normalisation seems to be

$$\bar{f}_{\beta\alpha}(t) = f_{\beta\alpha}(t) / I_\beta. \quad (6.13)$$

These functions obey

$$\bar{f}_{\beta\alpha}(0) = 0 \quad \bar{f}_{\beta\alpha}(\infty) = 1 \quad (6.14)$$

and are independent of detector parameters. Any deviation of  $\bar{f}_{\beta\alpha}(t)$  from unity then represents a genuine correlation between the emission of an  $\alpha$  and a  $\beta$  photon, irrespective of their detection. For correlations between circularly polarised photons we then find

$$\bar{f}_{\pm\pm}(t) = g_-(t) / n_e \quad (6.15)$$

$$\bar{f}_{\pm\mp}(t) = g_+(t) / n_e \quad (6.16)$$

and whenever a linearly polarised photon is involved, we obtain

$$\bar{f}_{\beta\alpha}(t) = \frac{1}{2}(g_+(t) + g_-(t)) / n_e. \quad (6.17)$$

Expressions (6.15)–(6.17) in combination with the explicit forms (6.9) and (6.10) constitute the central result of this paper. Figure 4 illustrates typical behaviour of the correlation functions.

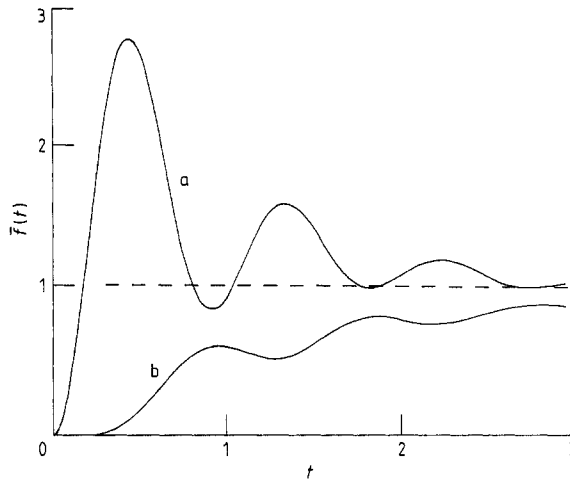


**Figure 4.** Two-photon correlation function  $\bar{f}_{\pm\mp}(t)$  (curve a) and  $\bar{f}_{\pm\pm}(t)$  (curve b). Frequencies will be given in units of the free-space Einstein coefficient  $A_f$ , time in units of  $1/A_f$  and the atom-surface distance  $h$  in wavelengths  $2\pi c/\omega_0$ . For this plot we take  $\Delta=0$ ,  $h=0.3$ ,  $\lambda=1.4$  and  $|\Omega_0|=7$ . Oscillations occur with a frequency  $|\Omega_0|$  (Rabi oscillations). We notice that  $\bar{f}_{\pm\mp}(t)$  can considerably exceed its long-time value, which implies that the probability for the detection of a  $\pm$  photon just after the emission of a  $\mp$  photon is larger than the uncorrelated probability for the detection of a  $\pm$  photon. In other words, the first emission enhances the probability for the second one. The probability for the emission of a  $\pm$  photon at time  $t$  after the emission of a similar photon at time zero is always significantly smaller than the uncorrelated probability, as shown by curve b. These strong correlations between photons with the same helicity are a consequence of the fact that in between the two emissions a three-photon process must occur, as explained in the text.

### 7. Short-time behaviour

Essential features of the photon correlation functions can readily be understood from an interpretation of figure 2 (Cohen-Tannoudji and Reynaud 1979). To this end we first recall that  $f_{\beta\alpha}(t)$  equals the probability for the detection of a  $\beta$  photon at time  $t$ , after the detection of an  $\alpha$  photon at time zero, independent of possible detections in between. For long delay times  $t$  there will be many photon emissions in between the detections of  $\alpha$  and  $\beta$ , and any correlation will be erased, which is expressed by  $f_{\beta\alpha}(\infty) = I_\beta$ . Therefore, the correlations between two successive photons are displayed in the short-time behaviour of the correlation functions. We have already found that  $g_{\pm}(0) = 0$  and from an expansion of  $\tilde{g}_{\pm}(s)$  around  $s = \infty$  we find the behaviour of  $g_{\pm}(t)$  around  $t = 0$ . It appears that the first non-vanishing derivatives are

$$g_+^{(2)}(0) = |\Omega_0|^2/2 \quad (7.1)$$

$$g_-^{(5)}(0) = \frac{2}{5} A_{\parallel} (|\Omega_0|^2/2)^2. \quad (7.2)$$

Consider first  $f_{+-}(t)$  which is proportional to  $g_+(t)$ . Emission of the  $-$  photon corresponds to a transition from  $|e-\rangle$  to  $|g+\rangle$  (figure 2), and the subsequent emission of the  $+$  photon is brought about by a decay from  $|e+\rangle$  to  $|g-\rangle$ . After the first emission the atom is in state  $|g+\rangle$ , which prohibits the emission of the second photon, for which the atom must be in state  $|e+\rangle$ . This implies  $g_-(0) = 0$ . Before the second emission can occur, the state  $|e+\rangle$  must be populated, and from figure 2 we see that this can be accomplished by the absorption of a single laser photon. On a short timescale, the probability for a stimulated transition must be proportional to the laser power  $|\Omega_0|^2$ , which explains why  $g_+(t)$  starts to deviate from zero according to equation (7.1). Next we consider the emission of two photons with the same polarisation, say  $+$ . An emission of a  $+$  photon corresponds to a  $|e+\rangle \rightarrow |g-\rangle$  transition so after the first  $+$  photon the atom is in state  $|g-\rangle$ . But now we notice that the laser cannot populate the state  $|e+\rangle$ ,

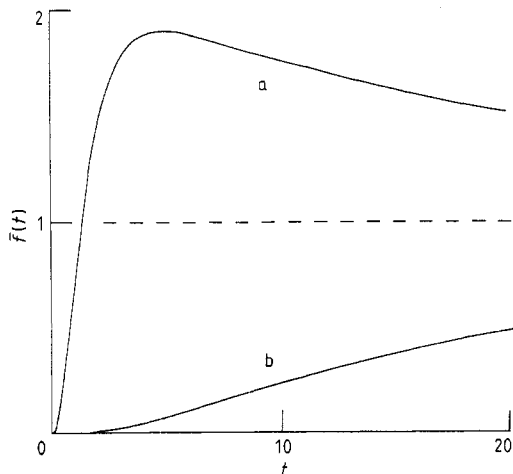


**Figure 5.** Same as figure 4, but with parameters  $\Delta = 0$ ,  $h = \infty$ ,  $\lambda = 1$  and  $|\Omega_0| = 0.3$ . These typical low-intensity curves (small  $|\Omega_0|$ ) show no Rabi oscillations. The extremely slow approach of  $\tilde{f}_{\pm\pm}(t)$  (curve b) to its long-time value reflects the fact that the emission of two circularly polarised photons with the same helicity requires the absorption of two laser photons in between. In this low-intensity picture, this second-order process in the laser power is very unlikely to happen.

starting from  $|g-\rangle$ . Absorption of a laser photon, which is the only excitation mechanism, amounts to a population of  $|e-\rangle$ . Then the atom must decay to  $|g+\rangle$ , under emission of a  $-$  photon, and subsequent excitation by the laser will finally result in a population of  $|e+\rangle$ . Then the second  $+$  photon can be emitted. In between two emissions of  $+$  photons, we have the stimulated absorption of two laser photons and a spontaneous emission of a circularly polarised photon, which explains the short-time behaviour of  $g_-(t)$ . Since the successive emission of two photons with the same helicity requires the intermediate absorption of two laser photons, this process is very unlikely to occur, especially for a low-intensity laser. In other words, these photon emissions are strongly correlated in comparison with the subsequent emission of a  $+$  and a  $-$  photon. This is illustrated in figure 5. Correlation functions which involve the emission of a linearly polarised photon ( $|e\pm\rangle \rightarrow |g\pm\rangle$  transitions) always acquire contributions from more than one pathway in figure 2. From (6.4) and (6.5) it follows that the correlation between a linear and a circular photon is a combination of two diagrams, whereas  $f_{00}(t)$  is determined by four processes. Because there is always a process which involves only the absorption of a single laser photon, every correlation with a linearly polarised photon behaves as  $g_+(t)$ , and hence is linear in the laser power.

## 8. Surface-enhanced correlations

Fluorescent emission is drastically affected by the presence of a metal surface if the atom-surface distance  $h$  becomes of the order of a wavelength or less. In the limit of small  $h$  the inverse lifetimes approach the values

$$A_{\perp} \rightarrow 2A_f \quad A_{\parallel} \rightarrow 0 \quad \text{for } h \rightarrow 0 \quad (8.1)$$

as follows from (2.2) and (2.3). Most dramatic is the disappearance of the Einstein coefficient  $A_{\parallel}$  for a parallel component of the dipole, which implies an infinite lifetime of an excited state (if there were not other decay channels). In this section we shall show how, in principle, the behaviour (8.1) can be obtained from a measurement of photon correlations.

Let us first consider the situation where  $\alpha$  or  $\beta$  (or both) is a linearly polarised photon. Then it follows from the explicit results in § 6 that the correlation function equals

$$\tilde{f}_{\beta\alpha}(s) = \frac{1}{4} |\Omega_0|^2 (\frac{1}{2}A + \lambda + s) / (n_e s D(s)). \quad (8.2)$$

Comparison with the result for a two-state atom in free space (Arnoldus and Nienhuis 1983) shows that this  $\tilde{f}_{\beta\alpha}(s)$  has exactly the same form. The lifetimes enter only through the combination  $A = A_{\perp}/3 + 2A_{\parallel}/3$ , and not as  $A_{\perp}$  and  $A_{\parallel}$  separately. If we assume the laser to be on resonance with the atomic transition frequency, monochromatic and sufficiently weak, then the Laplace inverse of (8.2) is easily found to be

$$\tilde{f}_{\beta\alpha}(t) = \{1 - \exp[-(A/2)t]\}^2. \quad (8.3)$$

For a free atom we have  $A = A_f$ , but if the atom approaches the surface we find from (8.1)

$$A \rightarrow A_{\perp}/3 = 2A_f/3 \quad \text{for } h \rightarrow 0 \quad (8.4)$$

which is smaller than  $A_f$ . Therefore, the typical correlation time  $(A/2)^{-1}$  is enhanced in the vicinity of the metal.

Far more pronounced is the change in correlation between circularly polarised photons with the same helicity. We set again  $\Delta = \lambda = 0$ , but now we assume that the laser field is relatively strong ( $|\Omega_0| \gg A$ ). Then the correlation functions will oscillate with the Rabi frequency  $|\Omega_0|$ . If we subsequently average over the fast oscillations (in comparison with the inverse lifetime), we find

$$\bar{f}_{\pm\pm}(t) = 1 - \exp[-(2A_{\parallel}/3)t]. \quad (8.5)$$

(Notice that there is no square, as in (8.3).) Hence the typical correlation time equals  $(2A_{\parallel}/3)^{-1}$  which can become arbitrarily large if the atom approaches the surface. This behaviour is depicted in figure 6.

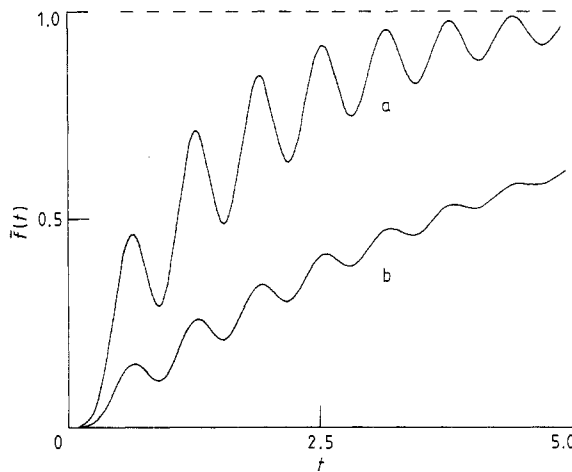


**Figure 6.** Plot of the two-photon correlation function  $\bar{f}_{\pm\pm}(t)$  for  $\Delta = 0$ ,  $\lambda = 0.5$  and  $|\Omega_0| = 10$ , for different values of the atom-surface distance. In curve a we have  $h = 1$ , and curve b represents  $h = 0.1$ , corresponding to an atom very close to the surface (although still far away in comparison with its own dimensions). Averaged over the fast Rabi oscillations, the exponential approach to the long-time values is governed by the correlation time  $(2A_{\parallel}/3)^{-1}$ , as follows from equation (8.5). For  $h = 1$  and  $h = 0.1$  we find from equation (2.3) that  $A_{\parallel} = 0.96$  and  $A_{\parallel} = 0.041$ , respectively.

## 9. Conclusions

We considered fluorescent emission by a laser-driven atom near a mirror and studied the temporal correlations between photons. It was shown that advantage can be taken of a polarisation-dependent measurement in such a way that only photons which are emitted in a specific transition are observed. Then correlations between these photons are governed by the Einstein coefficient for that particular transition. Already the ratio of the uncorrelated intensities of circularly and linearly polarised photons appeared to be determined by the ratio of  $A_{\parallel}$  and  $A_{\perp}$ , and not by any other optical parameters. A problem here is that this ratio is multiplied by a ratio of detector parameters, which only disappears if the efficiency equals unity. This would require a  $2\pi$  aperture (emission in a half space), which is probably not feasible in an experiment.

More promising are the normalised correlation functions  $\bar{f}_{\beta\alpha}(t)$ , which are independent of detector parameters. In other words, we can simply calibrate the intensity on  $\bar{f}_{\beta\alpha}(\infty) = 1$ . We elaborated on the situation of a  $j_e = j_g = \frac{1}{2}$  transition with an incident laser field propagating parallel to the surface and linearly polarised. The photon correlations for every combination of linear and circular detection were evaluated, and it appeared that the correlation time increases substantially if the atom-surface distance is diminished. In the case that at least one of the two photons is linearly polarised, the correlation time attains a value equal to  $\frac{3}{2}$  times its value for a free atom. For the situation of subsequent detections of two circularly polarised photons with the same helicity, the correlation time approaches infinity for  $h \rightarrow 0$ . We conclude that the presence of a metal surface enhances the correlations considerably, which should be amenable to observation. Figure 7 illustrates the enhancement for the two aforementioned cases.

A measurement of  $\bar{f}_{\pm\pm}(t)$  would essentially determine  $A_{\parallel}$ , according to (8.5). The obvious advantage is that  $A_{\parallel}$  changes significantly, and possibly by some orders of magnitude. The question can be raised as to whether it is feasible to design a similar geometry in which  $A_{\perp}$  plays the crucial role. To this end we recall that the essential correlation in  $\bar{f}_{\pm\pm}(t)$  is brought about by the necessary intermediate photon, which is emitted in the transition  $|e-\rangle \rightarrow |g+\rangle$  for  $\bar{f}_{++}(t)$  and in  $|e+\rangle \rightarrow |g-\rangle$  for  $\bar{f}_{--}(t)$ . Now suppose we irradiate the atom by a laser in normal incidence (along the  $z$  axis) and with linear polarisation. Then it follows from (3.9) that photon absorptions only cause transition from  $|g-\rangle$  to  $|e+\rangle$  and from  $|g+\rangle$  to  $|e-\rangle$ . We leave the detectors and polarisers the same. Assume the first photon (at  $t = 0$ ) is a  $+$  photon. Then the atom is in state

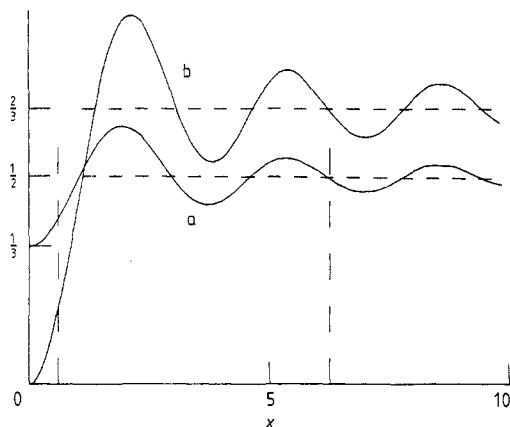


**Figure 7.** Inverse correlation times for the detection of two polarised photons as a function of  $x = \omega_0 h/c$ . Curve a represents  $A/2$ , which pertains to the case where at least one of the photons is linearly polarised (equation (8.3)). Curve b denotes  $2A_{\parallel}/3$ , which is the inverse correlation time for  $\bar{f}_{\pm\pm}(t)$  (equation (8.5)). For  $h \rightarrow 0$ , curve a approaches  $\frac{1}{3}$ , which is a factor of 1.5 less than its value for free atoms (dotted line at  $\frac{1}{2}$ ). Curve b, however, tends to zero for  $h \rightarrow 0$ , which implies an infinite correlation time. The vertical dotted lines indicate the points where the atom-surface distance equals a tenth and a whole wavelength, which corresponds to curves b and a in figure 6, respectively. It is seen from this figure that for  $h$  less than about 20% of a wavelength, the correlation times are always larger than their values for free atoms, whereas for larger distances the correlation times oscillate around their values for  $h \rightarrow \infty$ . Therefore, observation of surface-enhanced correlations, or equivalently, suppressed spontaneous decay, requires atom-surface distances of less than 20% of a wavelength.

$|g-\rangle$  at  $t = 0$ . Laser excitation, which is necessary for a subsequent emission, can then only populate  $|e+\rangle$ . Spontaneous decay afterwards produces a  $+$  photon or a  $0$  photon. Emission of a  $-$  photon, however, is prohibited since  $|e-\rangle$  is not populated. The only way to obtain a  $-$  emission is after a  $0$  emission ( $|e+\rangle \rightarrow |g+\rangle$  transition) and a laser-photon absorption ( $|g+\rangle \rightarrow |e-\rangle$ ). Then the inevitable intermediate spontaneous emission is a  $0$  emission, with Einstein coefficient  $A_{\perp}/3$ . Therefore, this configuration yields correlations with  $A_{\perp}/3$  in  $\bar{f}_{\pm\pm}(t)$ .

### Acknowledgments

This research was supported by the Office of Naval Research and the Air Force Office of Scientific Research (AFSC), United States Air Force, under Contract F49620-86-C-0009.

### References

- Agarwal G S 1974 *Phys. Rev. Lett.* **32** 703  
 — 1975 *Phys. Rev. A* **12** 1475  
 — 1978 *Phys. Rev. A* **18** 1490  
 Allen L and Eberly J H 1975 *Optical Resonance and Two-Level Atoms* (New York: Wiley)  
 Arnoldus H F and George T F 1987 *Phys. Rev. A* in press  
 Arnoldus H F and Nienhuis G 1983 *Opt. Acta* **30** 1573  
 Barton G 1974 *J. Phys. B: At. Mol. Phys.* **7** 2134  
 Cohen-Tannoudji C 1977 *Frontiers in Laser Spectroscopy, Proc. 27th Les Houches Summer School* ed R Balian, S Haroche and S Liberman (Amsterdam: North-Holland) p 3  
 Cohen-Tannoudji C and Reynaud S 1979 *Phil. Trans. R. Soc. A* **293** 223  
 Dagenais M and Mandel L 1978 *Phys. Rev. A* **18** 2217  
 Dalibard J, Dupont-Roc J and Cohen-Tannoudji C 1982 *J. Physique* **43** 1617  
 — 1984 *J. Physique* **45** 637  
 Drexhage K H 1974 *Progress in Optics* vol XII, ed E Wolf (Amsterdam: North-Holland) p 165  
 Glauber R J 1965 *Quantum Optics and Electronics* ed C DeWitt, A Blandin and C Cohen-Tannoudji (New York: Gordon and Breach)  
 Goy P, Raimond J M, Gross M and Haroche S 1983 *Phys. Rev. Lett.* **50** 1903  
 Huang X Y and George T F 1984 *J. Phys. Chem.* **88** 4801  
 Huang X Y, Lin J and George T F 1984 *J. Chem. Phys.* **80** 893  
 Hulet R G, Hilfer E S and Kleppner D 1985 *Phys. Rev. Lett.* **55** 2137  
 Jhe W, Anderson A, Hinds E A, Meschede D, Moi L and Haroche S 1987 *Phys. Rev. Lett.* **58** 666  
 Kelley P L and Kleiner W H 1964 *Phys. Rev.* **136** A316  
 Kimble H J, Dagenais M and Mandel L 1977 *Phys. Rev. Lett.* **39** 691  
 — 1978 *Phys. Rev. A* **18** 201  
 Kleppner D 1981 *Phys. Rev. Lett.* **47** 233  
 Lenstra D 1982 *Phys. Rev. A* **26** 3369  
 Lin J, Huang X Y and George T F 1983 *Solid State Commun.* **47** 63  
 Milonni P W, Acherhalt J R and Smith W A 1973 *Phys. Rev. Lett.* **31** 958  
 Milonni P W and Knight P L 1973 *Opt. Commun.* **9** 119  
 Morawitz H 1969 *Phys. Rev.* **187** 1792  
 Paul H 1982 *Rev. Mod. Phys.* **54** 1061